



Contents lists available at ScienceDirect

Chemical Physics Letters

journal homepage: [www.elsevier.com/locate/cplett](http://www.elsevier.com/locate/cplett)

## Learning from evolutionary optimization by retracing search paths

Peter van der Walle<sup>a,\*</sup>, Janne Savolainen<sup>b</sup>, L. Kuipers<sup>a,b</sup>, Jennifer L. Herek<sup>b</sup><sup>a</sup>FOM Institute for Atomic and Molecular Physics [AMOLF], Science Park 113, 1098 XG Amsterdam, The Netherlands<sup>b</sup>Optical Sciences Group, Department of Science and Technology, MESA+ Institute for Nanotechnology, University of Twente, 7500 AE Enschede, The Netherlands

### ARTICLE INFO

#### Article history:

Received 20 May 2009

In final form 14 October 2009

Available online xxxxx

### ABSTRACT

Evolutionary search algorithms are used routinely to find optimal solutions for multi-parameter problems, such as complex pulse shapes in coherent control experiments. The algorithms are based on evolving a set of trial solutions iteratively until an optimum is reached, at which point the experiment ends. We have extended this approach by recording the best solution in each iteration and subsequently applying these to a modified system. By studying the shape of the learning curves in different systems, features of the fitness landscape are revealed that aid in deriving the underlying control mechanisms. We illustrate our method with two examples.

© 2009 Elsevier B.V. All rights reserved.

### 1. Introduction

One of the central goals of coherent control is to extract new insights into molecular photophysical processes, by studying the pulse shapes that can effectively steer a system [1]. For the control of complex systems, in which many pathways compete, a broad bandwidth and a high spectral resolution are required to encode individual phases for the different pathways. For this purpose, liquid crystal pulse shapers have been developed, in which a mask containing hundreds of pixels spans the laser spectrum in the fourier-plane of a 4-f geometry [2]. With this many degrees of freedom, finding an effective control pulse is a difficult task. Hence, the pulse shaper is often incorporated in a learning loop, guided by an evolutionary algorithm, in order to find the optimal pulse shape for the control task at hand [3]. The loop optimizes a single experimentally determined feedback value, the fitness. While these learning loops may easily converge on pulse shapes with high yields, the resulting optimal pulse is often exceedingly complex. The complexity of the optimal pulse shape tends to impede the interpretation of the mechanism underlying the control.

Here we report a simple and general technique that supplements learning loop experiments and provide a handle for interpretation. The method is based on recording and saving the pulse shapes along a learning curve and subsequently repeating the measurement of the fitnesses corresponding to the application of these pulses on the system of interest. In the repeated measurements, a single parameter in the system is systematically varied in order to study its effect on the shape of the learning curve and/or optimization yield.

Fig. 1 represents schematically two systems with slightly different fitness landscapes (zooming in at a peak). An optimization

experiment is performed on system 1, ending at a maximum for this system. Then, using the retracing strategy, the pulse shapes recorded along the learning curve of this optimization are reapplied and measured on system 2. The difference in the shape of the resulting learning curve shows directly that the fitness landscapes cannot be compared. If random pulse shapes would be used instead, they are likely to fall outside of the peak for both systems, such that the comparison of the landscapes would be inconclusive.

We will illustrate how this method can be applied to gain insight into the system with two examples. First, using an artificial light harvesting complex in which we showed control over energy flow pathways [4], we will use the retracing strategy with varied laser fluence to distinguish two different control mechanisms. In the second example, the stimulated emission from a solvated dye was controlled [5], and by retracing the learning curve in different solvents we extracted insight on the effect of the surrounding environment. The retracing strategy is used to extend the range of solvents to a polar solvent, in which a different mechanism is observed.

Our method does not depend on the specific search algorithm. The only requirement is that it can successfully optimize a selected fitness value. We used the CMA-ES with weighted recombination for our optimizations [6]. The algorithm was setup to use a generation containing 40 pulse shapes of which the best 20 were recombined, weighted by their fitness value, into a new parent for the next generation. Due to this large number of pulse shapes taken in the recombination, the optimization is extremely robust to noise on the measured fitness value [7].

The phase function on the mask was described by the sum of three spline interpolants. A coarse spline with a spacing of 40 pixels and a range of  $3\pi$ , a spline with a spacing of 20 pixels and a range of  $1.5\pi$  and a fine spline with a spacing of 10 pixels and a range of  $.75\pi$ . The initial step-size was set to 10% of the range of the parameters.

\* Corresponding author. Fax: +31 207547290.

E-mail address: [p.v.d.walle@amolf.nl](mailto:p.v.d.walle@amolf.nl) (P. van der Walle).

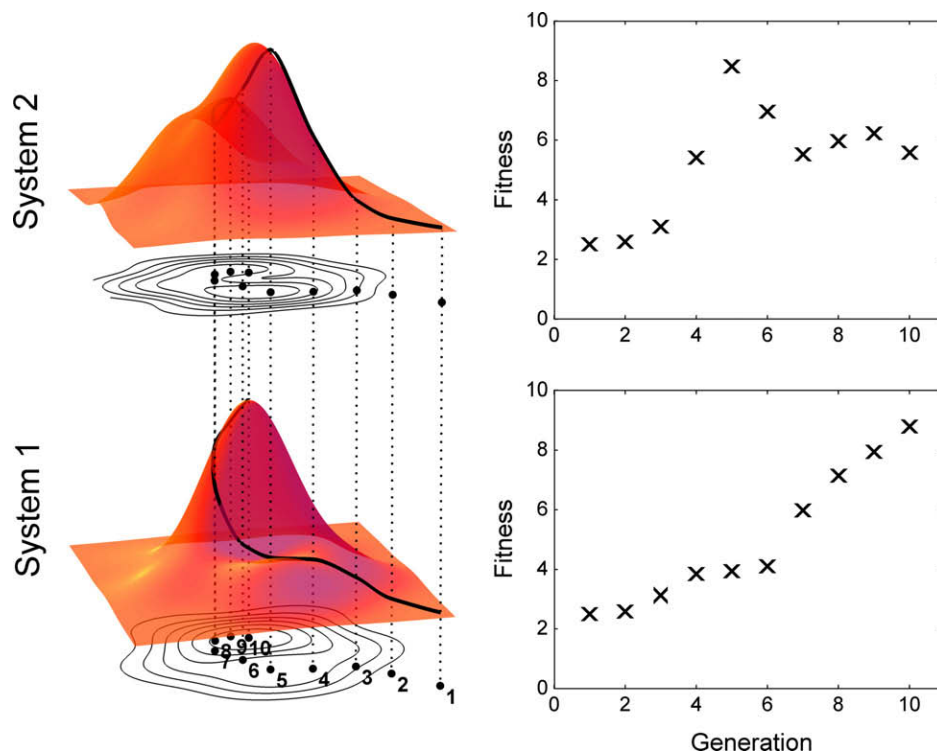


**Fig. 1.** Fitness landscapes (left) are compared by sampling with fixed pulse shapes. The pulse shapes are chosen along the learning curve of a successful optimization (right) to ensure a difference in response between the pulse shapes.

Both experiments use a pump–probe setup with a shaped pump pulse and an unmodulated white light probe pulse [8]. The feedback signal for the evolutionary algorithm is calculated by integrating a spectral window in a transient absorption spectrum, measured at a fixed time delay. In both examples only the phase of the pulse is modulated, leaving the pulse energy constant.

## 2. Distinguishing control mechanisms

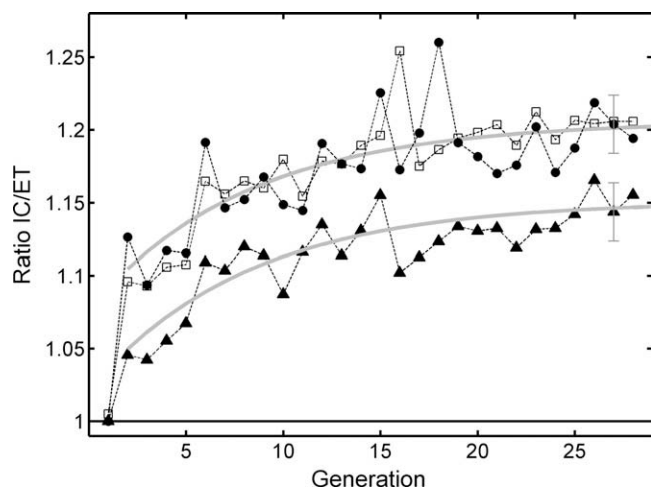
The first sample is an artificial light-harvesting complex that closely mimics the early-time photophysics of a natural light-harvesting protein (LH2) [8]. The complex consists of a single donor (carotenoid) and acceptor (porphyrin) moiety [9], thus significantly reducing the structural complexity compared to LH2 [10]. In the initial coherent control experiment [4] the target objective was to manipulate the branching ratio between the functional energy transfer (ET) channel and the internal conversion (IC) loss channel after excitation of the donor at 510 nm. The signals belonging to ET and IC were resolved from the transient spectrum measured at 8 ps time delay and their ratio was used as feedback for the optimization. The signature of the ET is a negative band at 700 nm, while a positive band around 610 nm is used as a measure of the IC. These bands correspond to the bleach of the porphyrin moiety and excited state absorption from a lower lying state in the carotenoid, respectively.

Fig. 2 shows the learning curve from the original optimization (circles) having a total increase of the IC/ET ratio of some 20%: an initial jump of  $\sim 10\%$  plus a gradual learning part providing an additional 10% improvement. Using the retracing strategy, we reapplied the pulse shapes of this learning curve, using 'identical' starting pulses (i.e. the same energy and spectral bandwidth) prepared two days later (open squares). With the exception of a few outliers caused by occasional laser instabilities, the agreement between the curves is good, which verifies the reproducibility of the

experiment. Note that the learning curve presented in Fig. 2 resulted from one of many closed-loop optimizations aimed at increasing the ratio IC/ET. Despite subtle variations, the learning curves were all found to share two characteristic features: an initial 'jump', followed by a further, gradual enhancement.

To allow for the possibility of multi-photon control schemes, the experiments on the light-harvesting complexes were performed using laser fluences that partially saturate the carotenoid  $S_0 \rightarrow S_2$  transition. As a result, a trivial control mechanism in which partial saturation is avoided simply by stretching the pulse in time produces the observed jump in the learning curves, but is not the cause of the subsequent gradual growth of the IC/ET ratio, as verified by repeating the measurement of the fitness curve with varying laser fluences. Fig. 2 also shows the learning curve retraced with only half of the original fluence (now 250 nJ, triangles). Fitting the data with a monotonically increasing function, we find that the same curve fits both measurements when offset to the first generation after the jump (Fig. 2, grey lines). This result shows that the jump and the 'learning' part have markedly different fluence dependencies: the initial jump decreases to approximately half of its amplitude when the fluence is halved, whereas the increase in the IC/ET ratio remains the same for the learning part of the curve ( $\sim 10\%$ ).

To better understand the scaling with excitation fluence, we simulated the saturation of the  $S_0 \rightarrow S_2$  transition to find out the role it plays in the measured IC and ET signals, and in the control results. In general, using a pulse shape that is stretched in time will give the photons in the trailing end of the pulse a probability to re-excite molecules that have had time to relax back to the ground state after transferring their energy to the acceptor. In this case, the excited state lifetime is on the order of 100 fs [8], hence a stretched pulse at high laser fluence can significantly increase the number of excitation processes, leading to an increase in the measured signal compared to the short pulse. Since the pulse analysis of the optimizations revealed a pulse-train structure [4], we



**Fig. 2.** Learning curve for the original optimization (circles) and two retraced curves, one at the original laser fluence (squares) and one at half the fluence (triangles).

simulated the magnitude of the IC and ET signals using a pulse train with 7 sub-pulses together with the experimental saturation curves of IC and ET (Fig. 3, inset). The simulation was made using an incoherent model of the dyad derived by fitting the transient absorption surface measured via pump-probe [8]. Note that, in the limit of a transform-limited excitation pulse, the same transition (carotenoid  $S_0 \rightarrow S_2$ ) is responsible for the saturation of both signals and an increase in the signal of IC brings a concomitant increase in the ET signal. However for the simulated shaped pulses, Fig. 3 shows that the ratio IC/ET increases as a function of the sub-pulse spacing. The origin of the variation of the IC/ET ratio with pulse separation is the fast energy transfer within the dyad. The donor passes its energy quickly to the acceptor, after which the donor can be re-excited. The re-excitation only increases the signal in the IC band, as the level representing the ET band is long-lived.

The original optimization was made with a pulse energy of 500 nJ per pulse. At this and lower energies, the IC/ET ratio increases nearly linearly with pulse separation. With the used parametrization for the phase function on the pulse shaper, a random pulse will have a multi-pulse structure with an envelope cor-

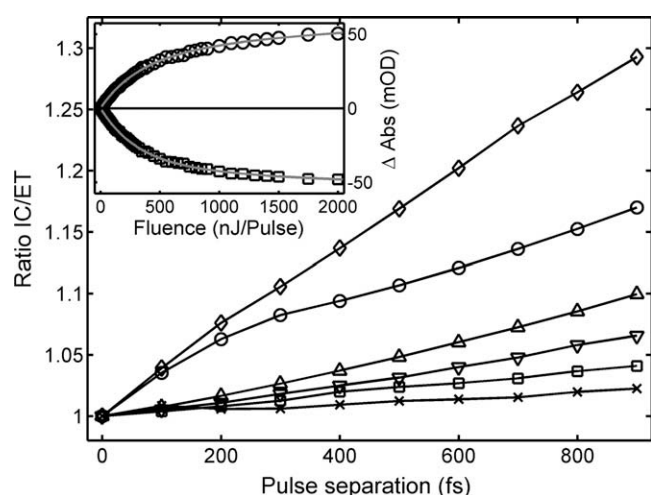


**Fig. 3.** Simulated ratio IC/ET as a function of pulse separation with increasing pulse energies: 50, 100, 250, 500, 1000, and 2000 nJ/pulse (asterisk, square, delta, triangle, circle, and diamond, respectively). Inset: Experimental saturation curves with TL pulse for the IC (circle) and ET (square) signals and exponential fit (grey lines).

responding to a train of 7 pulses with sub-pulse spacing of about 900 fs. The curve corresponding to 500 nJ/pulse shows a 10% increase in the IC/ET ratio at this spacing, consistent with the initial jump observed in the optimization.

Due to the random starting position of the search algorithm, the first pulse shapes will invariably be much longer than the transform-limited pulse, thereby creating an increase in the fitness via a trivial and *incoherent* control mechanism that merely avoids saturation. The subsequent learning part has a different scaling with excitation energy than the initial jump. In fact, the relative increase of the fitness in this part of the curve does not depend on the laser power. This scaling cannot be explained using the incoherent model of the dyad and it originates from an active *coherent* control mechanism over the branching of the energy flow (see [8]).

### 3. Comparing fitness landscapes and discriminating mechanisms

We now turn to a second example, in which we demonstrate how repeated measurements can be used to compare fitness landscapes. We studied the control of the stimulated emission from Coumarin 6. The original optimization was made in cyclohexane. As feedback, signal from an integrated spectral window (510–595 nm) from a transient absorption spectrum measured at 1 ns delay was used, corresponding to the stimulated emission band of the dye. The excitation pulse energy was 300 nJ/pulse and the spectrum centered around 475 nm, in the red tail of the absorption spectrum. The learning curve of the optimization performed in cyclohexane was remeasured in a range of solvents (the non-polar hexane, octane, decane and polar acetone), and the effect of the solvent on the fitness landscape was derived from the shapes of the obtained curves.

The fitness curves for the repeated optimizations in the different solvents were normalized to the fitness of the transform-limited pulse, so that the yield of the control could be compared directly (Fig. 4). To test if the fitness landscapes are topologically the same, we fit the curves simultaneously. One curve was described directly by the number of fitness values, while the other curves were described by the same values multiplied by a scaling factor. Taking into account the noise ( $\sim 2\%$  for decane and octane,  $\sim 5\%$  for hexane due to a lower solubility) the  $\chi^2$  is 1.3. In order to test our fit procedure, we simulated data sets based on a model

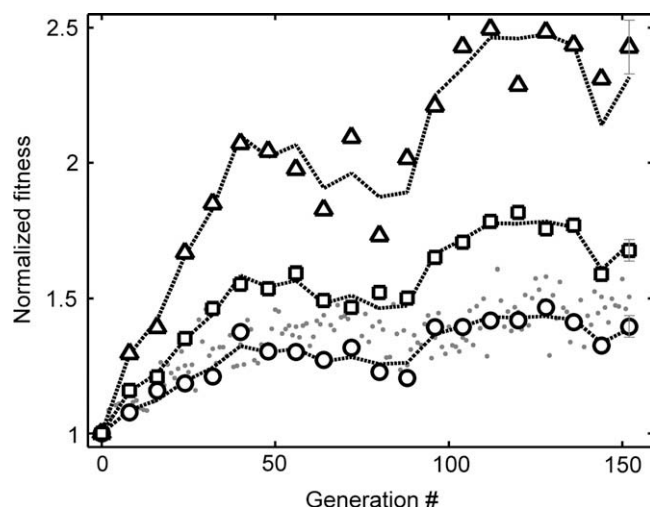


**Fig. 4.** Normalized fitness curves for the optimization of stimulated emission of Coumarin 6 in cyclohexane (grey dots), remeasured in different solvents, hexane (triangles), octane (squares), and decane (circles). The dashed lines are the result of a global fit that describes the curves with the same values, only scaled in amplitude.

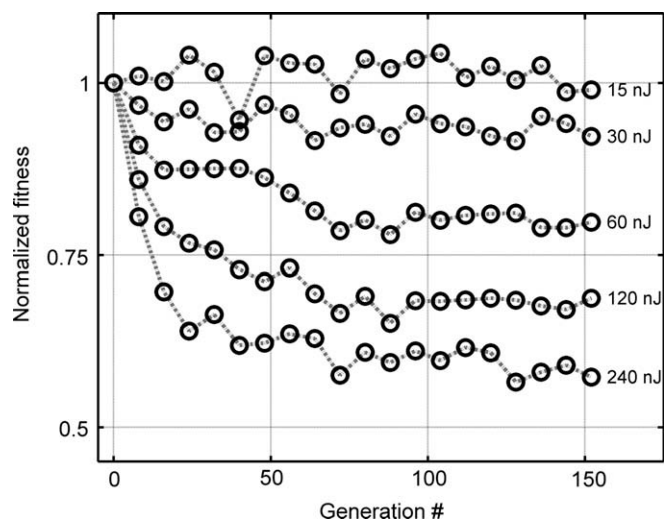


**Fig. 5.** Normalized fitness curves of the optimization in cyclohexane, remeasured in acetone at varying excitation pulse energies. The stimulated emission is reduced instead of enhanced in this solvent, especially at increasing pulse energy.

in which the shapes of different landscapes vary only by an amplitude scaling factor. The test data resulted in a distribution of  $\chi^2$  values with 95% of the values lower than 1.7. As the  $\chi^2$  for the fit to the experimental data is well below 1.7, this model clearly describes the data very well. The similarity in topology of the fitness landscapes shows that the photophysics are only weakly perturbed by the non-polar solvation, and that the features of the fitness landscapes are the same for all solvents.

In contrast, when the fitness curve obtained from the optimization in cyclohexane is remeasured with the dye dissolved in acetone—a polar solvent—the shape of the curve changes dramatically (Fig. 5). At low pulse energy there is no effect on the stimulated emission for any pulse shape along the curve. At increasing pulse energy, the direction of the fitness curve is reversed; instead of increasing, the stimulated emission is decreased by the shaped pulses. This effect is due to the shape of the optimal pulse—a down-chirp [5]—that limits the excitation via a 2-photon pump-dump process [11]. The observation of this non-linear effect is due to the significant red shift of the absorption spectrum of the dye in acetone, such that the peak of the absorption cross-section now overlaps with the laser spectrum. The excitation is well outside the linear regime for the higher laser fluences, facilitating the pump-dump mechanism.

The retracing technique is a powerful method to detect differences in the control mechanism upon variation of the experimental conditions. Independent optimizations can produce dramatically different learning curves, even when run with identical conditions. Furthermore, if after different optimizations, different optimal pulse shapes are found, it is possible that the algorithm was simply attracted to a different (local) maximum, while the global fitness landscapes are the same. Using the retracing technique, the landscapes of different systems can be consistently sampled and compared, allowing discrimination of control mechanisms by inspection of remeasured learning curves.

In the case of the solvated dye, the remeasured learning curves indicate that the fitness landscape has the same shape in all tested non-polar solvents and that the result of the optimal pulse shape can be compared directly. Although in some cases comparing the fitness of the transform-limited pulse to that obtained with the best pulse may suffice in bringing further understanding of the control [12], we have shown that the shape of the learning curve can provide additional information: the saved pulse shapes map out a path through the multidimensional search space and the fitness curve depicts the value of a chosen physical parameter along this path. Generally, variations in the shape of the fitness curve in the repeated experiments indicate that the fitness landscape is different, and therefore the underlying physical control mechanism has changed.

We have presented a simple technique that complements evolutionary control experiments and that can ultimately be employed to utilize the obtained optimization results to extract further information on the molecular mechanisms and how they are influenced by external parameters. The power of repeated measurements has been demonstrated with two examples. A trivial and a non-trivial learning part in the control of the artificial light-harvesting complex have been separated. The difference between the photophysics in polar and non-polar solvents was observed from the learning curve and, for the non-polar solvents, a clear trend has been identified in the optimization of stimulated emission from a dye. These examples show how the technique enables a direct comparison of the outcome of an optimization when a single parameter is systematically varied. In addition, the repeated measurements verify the reproducibility of the optimization results. In this paper, we have applied the technique to a coherent control experiment. However, it can also be applied in any other optimization experiment based on a stochastic search algorithm.

### Acknowledgements

This work is part of the research program of the 'Stichting voor Fundamenteel Onderzoek der Materie (FOM)', which is financially supported by the 'Nederlandse organisatie voor Wetenschappelijk Onderzoek (NWO)'.

### References

- [1] H. Rabitz, R. de Vivie-Riedle, M. Motzkus, K. Kompa, *Science* 288 (2000) 824.
- [2] A.M. Weiner, *Rev. Sci. Instrum.* 71 (2000) 1929.
- [3] R.S. Judson, H. Rabitz, *Phys. Rev. Lett.* 68 (1992) 1500.
- [4] J. Savolainen et al., *Proc. Natl. Acad. Sci. USA* 105 (2008) 7641.
- [5] P. van der Walle, M.T.W. Milder, L. Kuipers, J.L. Herek, *Proc. Natl. Acad. Sci. USA* 106 (2009) 7714.
- [6] N. Hansen, A. Ostermeier, *Evol. Comput.* 9 (2001) 159.
- [7] R. Fanciulli, L. Willmes, J. Savolainen, P. van der Walle, T. Bäck, J.L. Herek, in: N. Monmarché, E.-G. Talbi, P. Collet, M. Schoenauer, E. Lutton (Eds.), 8th International Conference on Artificial Evolution, Lecture Notes in Computer Science, vol. 4926, Springer, Tours, 2007.
- [8] J. Savolainen et al., *J. Chem. Phys.* B 112 (2008) 2678.
- [9] A. Macpherson et al., *J. Phys. Chem.* B 106 (2002) 9424.
- [10] G. McDermott, S.M. Prince, A.A. Freer, A.M. Hawthornthwaite-Lawless, M.Z. Papiz, R.J. Cogdell, N.W. Isaacs, *Nature* 374 (1995) 517.
- [11] C.J. Bardeen, V.V. Yakovlev, J.A. Squier, K.R. Wilson, *J. Am. Chem. Soc.* 120 (1998) 13023.
- [12] V.I. Prokhorenko, A.M. Nagy, S.A. Waschuk, L.S. Brown, R.R. Birge, R.J.D. Miller, *Science* 313 (2006) 1257.